ACT3: A Putative Centractin Homologue in *S. cerevisiae* Is Required for Proper Orientation of the Mitotic Spindle

Sean W. Clark and David I. Meyer

Department of Biological Chemistry and the Molecular Biology Institute, University of California, Los Angeles, California 90024

Abstract. As part of our ongoing efforts to understand the functional role of vertebrate centractins, we have identified a new member of the actin-related family of proteins in the yeast *Saccharomyces cerevisiae* using a PCR-based approach. Consistent with the current nomenclature for actin-related proteins in yeast, we propose to denote this locus *ACT3*. The primary amino acid sequence of Act3p is most similar to canine and human α-centractin (73% similarity/54% identity). The sequence of a genomic clone indicates *ACT3* lies adjacent to and is transcribed convergently with respect to *FUR1* on chromosome VIII. Molecular genetic analysis indicates *ACT3* is represented by a single gene from which the corresponding mRNA is expressed at a low level compared to *ACT1*. Tetrad analysis of heterozygotes harboring a *TRP1* replacement of the *ACT3*-coding region indicates *ACT3* is nonessential for growth under normal conditions and at extremes of temperature and osmolarity. However, growth at 14°C indicates a spindle orientation defect similar to phenotypes recently described for yeast harboring mutations in actin, tubulin, or cytoplasmic dynein. Taken together, our data suggest that *ACT3* is the *S. cerevisiae* homologue of vertebrate centractins.

ACTIN is a major component of the eukaryotic cytoskeleton. In its filamentous form, actin is responsible for muscle contraction, cytokinesis, maintenance of cell morphology, cell motility, and organelle movement (Pollard and Cooper, 1986). Even between diverse species, actins form a cohesive group of highly conserved proteins in regard to their primary sequence, length, and function. In recent years, a large number of proteins related in primary sequence to actin have been identified (Herman, 1993). Unlike conventional actins, these actin-related proteins (ARPs)[1] form a heterogeneous group both in primary sequence, overall length, and the position of peptide insertions and deletions relative to actin. The location of ARP insertions have led some investigators to question the likelihood of ARP interaction with conventional actins and the possibility of polymer formation (Fyrberg and Fyrberg, 1993). Recently, actin was found to have a tertiary structure similar to that of HSC-70 and hexokinase (Flaherty et al., 1991; Bork et al., 1992). This has led to the suggestion, despite their distinct cellular roles, that these three proteins evolved from a common progenitor (Bork et al., 1992). Likewise, the diversity of the ARP family poses the question of whether ARPs share any functional relationship to conventional actins. It may be, that, aside from the conservation of residues involved in nucleotide binding and scaffolding for the tertiary structure, ARPs constitute a family of proteins in their own right, as distinct in function from conventional actins as HSC-70 and the sugar kinases. Accordingly, one focus of our research has been to clarify the functional relationship between certain actin-related proteins and conventional actins.

Unfortunately, the acquisition of functional details regarding this family of proteins has not progressed nearly as rapidly as new members and their homologues have been identified. ARPs have been found not only in fungi (Lees-Miller et al., 1992*a*; Schwob and Martin, 1992; GenBank Accession Number L21184; Harata et al., 1994; Plamann et al., 1994), but also in nematodes (J. Lees-Miller personal communication), fruit flies (Fyrberg and Fyrberg, 1993; Frankel et al., 1994), dogs (Clark and Meyer, 1992), cows (Tanaka et al., 1992; Paschal et al., 1993), and humans (Clark and Meyer, 1992; Lees-Miller et al., 1992*b*). In yeast, three ARPs have been identified, all of which, like conventional actin, are essential. In *Saccharomyces cerevisiae*, the product of the essential *ACT2* gene has been proposed to act late in the cell cycle, perhaps at cytokinesis (Schwob and Martin, 1992). ARPs identified in two other genetically tractable organisms, *Caenorhabditus elegans* and *Drosophila melanogaster*, have yet to be functionally or phenotypically characterized (Fyrberg and Fyrberg, 1993; Frankel et al., 1994).

In vertebrates, biochemical studies have found an ARP (centractin/actin-RPV, henceforth referred to as centractin) associated with two macromolecular complexes: the p150^{Glued}/dynactin complex (Lees-Miller et al., 1992*b*; Paschal et al., 1993) and a cytoplasmic chaperonin (Melki et al.,

Address all correspondence to David Meyer, Dept. of Biological Chemistry & Molecular Biology Institute, University of California, Los Angeles, CA 90024. Tel.: (310) 206-3122. Fax: (310) 206-5272.

1. *Abbreviation used in this paper*: ARP, actin-related proteins.

*Table I. Oligonucleotide Primers**

ARP-9	GGG ATG ATA TGG AAA AAA TWT GG	Sense
ARP-10R	GCA TAN CCT TCA TAW ATW GGW AC	Antisense
P17	TTA GTA GCA TAA TGT TCT GAA C	Sense
P18	CAC TTA GCG GAT CCA TTG GCT A (*Bam*HI)	Antisense
P19A	CTT TCA AAG AAT TCG GAC CAA A (*Eco*RI)	Sense
P20	CTG GTG CCC TCG AGA GAG GTC T (*Xho*I)	Antisense

* Synthesized as written. Underlined nucleotides indicate changes relative to plasmid pBScKS-YC2 sequence, to incorporate restriction sites. Introduced restriction sites are given in parentheses.

1993). The p150^{Glued}/dynactin complex affects the activity of cytoplasmic dynein while the cytoplasmic chaperonin appears to assist in the folding of centractin and γ-tubulin. Crude preparations of cytoplasmic dynein will bind vesicles and move them along microtubules (Schroer et al., 1989). However, when further purified, cytoplasmic dynein still binds to, but can no longer translocate, vesicles (Schroer and Sheetz, 1991). This assay has led to the biochemical characterization of a cytosolic complex capable of restoring vesicle movement to purified cytoplasmic dynein (Shroer and Sheetz, 1991). This dynein-activating complex has been designated as the p150^{Glued} (Holzbauer et al., 1991; Paschal et al., 1993) or dynactin (Gill et al., 1991) complex. The p150^{Glued}/dynactin complex consists of three major constituents having molecular masses of 45, 50, and 150 kD (Gill et al., 1991; Paschal et al., 1993). The 45-kD component is now known to be centractin (Lees-Miller et al., 1992*b*, Paschal et al., 1993) which contributes more than half of the complex's mass (Gill et al., 1991; Paschal et al., 1993). The 150-kD component has been cloned and partially characterized (Gill et al., 1991; Holzbaur et al., 1991). It is homologous to an essential *Drosophila* gene, *Glued*, which when mutant leads to pleiotropic developmental defects particularly evident in the eye (Meyerowitz and Kankel, 1978; Harte and Kankel, 1982; Garen and Kankel, 1983; Gill et al., 1991; Holzbaur et al., 1991). The 150-kD protein also shares similarity to CLIP-170, a microtubule-endocytic vesicle linkage protein (Pierre et al., 1992). The 50-kD protein has not yet been characterized. In contrast to the heterogenous size distribution of actin filaments, the p150^{Glued}/dynactin complex, and hence centractin, is monodisperse (Paschal et al., 1993). Immunofluorescence data using antibodies against two of the components, centractin and p150^{Glued} indicates a localization of the complex to the centrosome and cytoplasmic vesicles (Clark and Meyer, 1992, 1993; Gill et al., 1992; Paschal et al., 1993), a localization overlapping with that of cytoplasmic dynein (Gill et al., 1992). However, the role of centractin in this regulator of cytoplasmic dynein has not been clarified.

Recently, cytoplasmic dynein has been identified in the yeast *S. cerevisiae* (Eshel et al., 1993; Li et al., 1993). Surprisingly, dynein is not an essential gene and the only phenotype thus far identified does not involve vesicular trafficking. Instead, yeast lacking dynein have defects in mitotic spindle orientation and thus nuclear migration (Eshel et al., 1993; Li et al., 1993). However, despite its proposed role in the poleward movement of chromosomes (Sawin and Scholey, 1991), chromosome segregation occurs normally in dynein mutants (Eshel et al., 1993; Li et al., 1993). A similar spindle misorientation phenotype is found in yeast harboring mutations in actin (Palmer et al., 1992) and tubulin (Huffaker et al., 1988; Palmer et al., 1992).

Clearly, the actin-related protein family has grown rapidly since the discovery of the first nonconventional actin in yeast by Schwob et al. (1988). The size of this family presents a problem when comparing ARPs among different species. Fyrberg and Fyrberg (1993) have suggested classifying ARPs based on peptide insertions relative to conventional actins. However, relationships contingent on sequence similarities are most meaningful when borne out by functional similarity. Thus, we have initiated an effort to delineate the role of centractins through their characterization in the genetically-amenable organism, *S. cerevisiae.*

Materials and Methods

Media

S. cerevisiae were grown in YPD medium (1% bacto-yeast extract/2% bacto-peptone/2% dextrose) for routine work (Guthrie and Fink, 1991). For growth curves, SD medium (0.67% yeast nitrogen-base/2% dextrose) (Guthrie and Fink, 1991) plus Nutrient Mix (0.4% adenine, 0.2% histidine, 0.3% leucine, 0.2% uracil, 0.2% tryptophan, 0.3% lysine) was used. When selection was necessary, SD medium was used containing Nutrient Mix minus the appropriate nutrients. For sporulation, SPO plates were used (Guthrie and Fink, 1991). For *Escherichia coli* strain XLI-Blue (Stratagene Inc., La Jolla, CA) LB medium was used (Sambrook et al., 1989) and when required, ampicillin, IPTG, and XGAL were added to final concentrations of 100 μg/ml, 0.3 mM, and 50 μg/ml, respectively. For *E. coli* strain Y1090, NZY medium was used containing 0.2% maltose. λgt11 phage were grown on lawns of Y1090 on NYZ plates. 1.6% Bacto agar (Difco, Detroit, MI) was used to solidify all media as necessary, except NZY-Top agarose which was solidified with 1.6% agarose (GIBCO BRL, Gaithersburg, MD).

PCR Amplification of the ACT3 Fragment

Primers ARP-9 and ARP-10R (see Table I) were added at 50 pmol to a 100

Table II. Plasmids

pBScKS-YC1	3.1-kb genomic clone of *ACT3* in pBluescriptKS− at *Eco*RI
pBScKS-YC2	4.5-kb genomic clone of *ACT3* in pBluescriptKS− at *Eco*RI
pBScKS-910	276-bp PCR amplified product of primers ARP-9 and ARP-10R in pBluescriptKS− (ddT vector) at *Eco*RV
pBSKS-TRP1	1022 bp *TRP1 Ssp*I/*Stu*I fragment derived from plasmid YRp17, subcloned into pBluescriptKS+ at *Sma*I
pTRP17-20	*act3Δ1-366::TRP1* disruption/replacement plasmid

Table III. Saccharomyces cerevisiae Strains

	Genotype	Source
ABYS1	*MATα pra1 prb1 prc1 cps1 ade*	Toyn *et al.*, 1988
GPY278	*MATa/MATα leu2/leu2 ura3/ura3 his3-Δ200/his-Δ200 trp1-Δ901/trp1-Δ901 ade2/+ lys2/+*	G. Payne (University of California at Los Angeles)
W303	*MATa/MATα leu2-3,112/leu2-3,112 ura3-1/ura3-1 his3-11,15/his3-11,15 trp1-1/trp1-1 ade2-1/ade2-1 can1-100/can1-100*	Munn *et al.*, 1991
BY101	*GPY278 act3Δ1-366::TRP1/+*	This study
BY103	*GPY278 act3Δ1-366::TRP1/+*	This study
BY106	*W303 act3Δ1-366::TRP1/+*	This study
BY108	*W303 act3Δ1-366::TRP1/+*	This study
BY101-9A	*MATa leu2 ura3 his3-Δ200 trp1-Δ901 ade2 act3Δ1-366::TRP1* (segregant of BY101)	This study
BY101-9B	*MATα leu2 ura3 his3-Δ200 trp1-Δ901* (segregant of BY101)	This study
BY101-9C	*MATα leu2 ura3 his3-Δ200 trp1-Δ901 lys2* (segregant of BY101)	This study
BY101-9D	*MATa leu2 ura3 his3-Δ200 trp1-Δ901 ade2 lys2 act3Δ1-366::TRP1* (segregant of BY101)	This study
BY103-3A	*MATα leu2 ura3 his3-Δ200 trpl-Δ901* (segregant of BY103)	This study
BY103-8B	*MATα leu2 ura3 his3-Δ200 trp1-Δ901 act3Δ1-366::TRP1* (segregant of BY103)	This study
BY103-7C	*MATα leu2 ura3 his3-Δ200 trp1-Δ901 ade2 lys2 act3Δ1-366::TRP1* (segregant of BY103)	This study
BY103-7D	*MATa leu2 ura3 his3-Δ200 trp1-Δ901 ade2 lys2* (segregant of BY103)	This study
BY106-1A	*MATα leu2-3,112 ura3-1 his3-11,15 trp1-1 ade2-1 can1-100* (segregant of BY106)	This study
BY106-1B	*MATa leu2-3,112 ura3-1 his3-11,15 trp1-1 ade2-1 can1-100 act3Δ1-366::TRP1* (segregant of BY106)	This study
BY106-1C	*MATa leu2-3,112 ura3-1 his3-11,15 trp1-1 ade2-1 can1-100 act3Δ1-366::TRP1* (segregant of BY106)	This study
BY106-1D	*MATα leu2-3,112 ura3-1 his3-11,15 trp1-1 ade2-1 can1-100* (segregant of BY106)	This study
BY106-9B	*MATa leu2-3,112 ura3-1 his3-11,15 trp1-1 ade2-1 can1-100 act3Δ1-366::TRP1* (segregant of BY106)	This study
BY106-9C	*MATa leu2-3,112 ura3-1 his3-11,15 trp1-1 ade2-1 can1-100* (segregant of BY106)	This study
BY108-4B	*MATa leu2-3,112 ura3-1 his3-11,15 trp1-1 ade2-1 can1-100* (segregant of BY108)	This study
BY108-4C	*MATa leu2-3,112 ura3-1 his3-11,15 trp1-1 ade2-1 can1-100 act3Δ1-366::TRP1* (segregant of BY108)	This study
GX3087	*MATα arg1*	G. Payne
GX3088	*MATa arg1*	G. Payne

μl reaction containing 100 ng ABYS1 genomic DNA, 2.5 U Taq DNA polymerase (The Perkin-Elmer Corp., Norwalk, CT), 200 mM dNTPs (Pharmacia LKB Nuclear, Gaithersburg, MD) in a buffer containing 10 mM Tris–Cl, pH 8.8, 50 mM KCl, 1 mM DTT, 1.5 mM $MgCl_2$, and 0.001% gelatin. The reaction was cycled 35 times in a Perkin-Elmer Thermal Cycler at 94°C, 1 min (melting), 50°C, 1 min (annealing), 72°C, 30 s (polymerization). Reactions were started at 80°C, directly from ice. The amplified products were isolated from LMP-agarose (GIBCO BRL) gels using Gelase (Epicenter Technologies, Madison, WI) according to the manufacturer's protocol. Gel-purified amplification products were sequenced directly to confirm their identity and determine the degree of heterogeneity using the Cyclist Taq DNA Sequencing System (Stratagene Inc.) with the annealing temperature equal to that used in the initial amplification. To create plasmid pBScKS-910, the amplified product was cloned directly into pBluescriptKS− (Stratagene Inc.) at the *Eco*RV site by the ddT-Vector method (Holton and Graham, 1991). Transformation was by the $CaCl_2$ method (Sambrook et al., 1989). Transformants were screened on LB/amp/IPTG/XGAL plates and white transformants were confirmed directly by double-stranded sequencing, using the boiling lysis method of plasmid isolation (Ausubel et al., 1993). All oligonucleotides were synthesized on an Applied Biosystems 391A DNA synthesizer.

Probes

For library screening and for the genomic Southern of ABYS1 DNA, the 276 bp ARP9/10R fragment was liberated from plasmid pBScKS-910 at *Eco*RI/*Hin*dIII. For Northern and Southern blotting of diploid parental disruptants and their dissected tetrads, a 1719-bp *Xba*I/*Sac*I fragment was isolated from plasmid pBScKS-YC2 as an *ACT3* probe. Additionally, an *ACT1* probe was amplified from genomic ABYS1 DNA using PCR with primers from the second exon representing residues 18–345 (Gallwitz and Sures, 1980). The 985-bp *ACT1* PCR product was cloned into a ddT-vector and confirmed by sequencing. Then, a 740-bp *ACT1* probe was liberated with *Eco*RI and *Hin*dIII (*Hin*dIII cuts within the insert). All fragments were purified by agarose-gel electrophoresis, then cut out and run through a second gel of LMP-agarose from which they were finally isolated as above. Gel purified fragments were labeled by random priming (USB) with [α^{32}P]-dCTP (3000 Ci/mmol; NEN, Boston, MA) and purified away from unincorporated radionucleotide by spin chromotography through G-50 (Pharmacia LKB Nuclear) by standard methods (Sambrook et al., 1989).

Isolation and Sequencing of the ACT3 Genomic Clones, YC1 and YC2

A *S. cerevisiae* λgt11 genomic library (YL1001b; Clontech, Palo Alto, CA) was screened with the cloned PCR product, pBScKS-910, using standard methods (Sambrook et al., 1989). Two lambda phage clones were isolated and large scale preps made by the plate lysis method (Sambrook et al., 1989). Purified phage DNA was digested with *Eco*RI and the liberated fragments of 3.1 and 4.5 kb were subcloned into pBluescriptKS$^-$ producing plasmids pBScKS-YC1 and pBScKS-YC2, respectively (Table II). Nested exonuclease III deletions (Sambrook et al., 1989) were produced and both clones were sequenced entirely by double-stranded sequencing on both the sense and antisense strands. Clone pBScKS-YC1 was found to be encompassed by clone pBScKS-YC2, thus only the latter was used for further study.

Construction of the act3Δ1-366::TRP1 Disruption/Replacement Plasmid, pTRP17-20

Sequences flanking the region of *ACT3* to be deleted were amplified by PCR from plasmid pBScKS-YC2. The primers were designed so as to use naturally occurring restriction sites where possible and otherwise incorporate new sites with minimal changes in the nucleotide sequence (see Fig. 3). For the 5′ flanking region the primers were P17 and P18 and for the 3′ flanking region the primers were P19A and P20 (see Table I). Amplification parameters were 1 min 94°C, 1 min 50°C, 30 s 72°C for 25 cycles. The amplification products were isolated from agarose gels using a Spin-X column (Costar Corp., Cambridge, MA) (Volgelstein, 1987) and digested with the appropriate restriction enzyme. Plasmid pBSKS-TRP1 was digested at *Sac*I and *Bam*HI, gel purified and the P17/P18 amplification product was ligated in. The ligation product was transformed into XL1-Blue,

then plasmid DNA was reisolated by boiling lysis, confirmed by restriction digest, and cleaved with *Eco*RI and *Xho*I for insertion of the P19A/P20 amplification product. The completed plasmid, pTRP17-20, was isolated using a Midi Prep column (QIAGEN Inc., Chatsworth, CA). Plasmid pTRP17-20 was cleaved at *Sac*I and *Xho*I, then isolated from a LMP-agarose gel. The fragment was quantitated using a TKO 100 DNA fluorimeter (Hoefer Sci. Instrs., San Francisco, CA).

Disruption of the ACT3 Locus

Replacement was accomplished by the one-step method (Guthrie and Fink, 1991). Strains W303 and GPY278 (see Table III) were transformed by the LiOAc method (Ito et al., 1983) using 5 μg of the pTRP17-20 plasmid *Sac*I/*Xho*I fragment.

Southern and Northern Blotting

DNA was separated on 1% agarose gels in 1× TAE. RNA was added to three volumes of 59% formamide/1.2× MOPS/18% formaldehyde, heated 5 min at 68°C, then separated on 15% formaldehyde/1% agarose gels in 1× MOPS. Blotting was conducted by capillary transfer to ZetaProbeGT membranes (Bio Rad Labs, Hercules, CA). Gel preparation, transfer, blot fixation, hybridization, and stripping on were carried out according to the manufacturer. Blots were washed twice for 5 min at 65°C in 0.2× SSC/5%SDS then twice for 30 min at 65°C in 0.2× SSC/1%SDS. Blots were exposed to X-OMAT film (Kodak) with a single intensifying screen at −80°C.

Isolation of Genomic DNA, Total RNA, and Poly(A)$^+$ RNA

Genomic DNA and total RNA were prepared according to Rose et al. (1990). Poly(A)$^+$ RNA was selected on oligo-dT Cellulose (Boehringer Mannheim Corp., Indianapolis, IN) according to Sambrook et al. (1989).

Genetic Methods

All yeast growth was at 30°C unless otherwise noted. Sporulation and tetrad dissection were according to (Guthrie and Fink, 1991). Temperature sensitivity was scored by streaking on YPD plates at 14, 30, or 37°C; osmotic sensitivity was scored on YPD/1.5M KCl plates and grown at 30°C. Mating was tested by complementation using strains GX3087 or GX3088. Growth curves were conducted in SD media plus Nutrient Mix at 14, 30, or 37°C. Growth was measured by both absorbance at 600 nm (A_{600}) and directly by hemocytometer. Cultures were maintained below A_{600} = 1.1 by dilution into fresh media, preequilibrated to the appropriate temperature. In all cases, growth was initiated at 30°C until logarithmic phase was achieved, then cultures were shifted to the appropriate temperature by dilution into preequilibrated media.

Analysis of Yeast Morphology

For analysis of the yeast vacuole and endocytosis we utilized two methods. First we took advantage of the naturally fluorescent *ade2* fluorophore (Weisman et al., 1987; Guthrie and Fink, 1991). Wild type and *act3*Δ haploids were grown to stationary phase in YPD to accumulate the *ade2* fluorophore, then diluted into fresh media and grown until the density doubled. The *ade2* fluorophore was visualized on a Nikon Microphot-FXA with epifluorescent optics using the G filter set (EX510-560, DM580, and BA590). Alternatively, wild type and *act3*Δ haploids were grown to A_{600} = 0.25, 1 OD_{600} of cells was removed and resuspended in 100 μl of YPD containing 4–16 mg/ml Lucifer Yellow-CH (Fluka Chem Corp., Ronkonkoma, NY). The dye was allowed to accumulate 2 h at 30°C. Yeast were then washed three times in 1 ml ice-cold 50 mM sodium succinate/20 mM sodium azide, pH 5.0, then resuspended in 10 μl wash buffer according to the method of (Guthrie and Fink, 1991). Lucifer Yellow-CH was visualized with the B2 filter set (EX450-490, DM510, and BA520). Nuclear position was examined by DAPI staining. Yeast were grown to A_{600} = 0.4 at 30°C, then shifted to prechilled 14°C media or maintained at 30°C for 24 h in both cases. Cells grown continuously at 14°C produced equivalent results. 1 OD_{600} of cells were washed in dH_2O, then resuspended in 70% ethanol for 30 min at room temperature. Fixed cells were washed in dH_2O again, then resuspended in 100 μl of 0.5 μg/ml DAPI in dH_2O for 5–30 min followed by a final dH_2O wash. DAPI staining was visualized with the UV filter set (EX330-380, DM400, and BA420). Spindle orientation and microtubule morphology were analyzed using indirect immunofluorescence with the YOL1/34 rat mAb (SeraLab, Sussex, England). Yeast were grown as for nuclear position analysis, fixed in 4% formaldehyde at 14°C for 1 h, then 16 h in 4% paraformaldehyde at 30°C as described (Guthrie and Fink, 1991). Cell walls were removed with 10U/OD_{600} oxalyticase (Enzogenetics, Corvallis, OR) and a 1/40 dilution of Glusulase (New England Nuclear). Fixed yeast were attached to slides with a 1 mg/ml solution of polylysine (Sigma Chem. Co., St. Louis, MO). The YOL1/34 antibody was used at 1:50. An FITC-conjugated goat anti-rat secondary (Jackson ImmunoResearch Labs., Inc., West Grove, PA) was absorbed against fixed wild-type yeast at 1.5 μg antibody per OD_{600} yeast, then used at 1:200. FITC fluorescence was visualized with the B2 filter set. TriX-400 and Ektachrome 400 (Kodak) were used to photograph yeast. Yeast cultures were scored for the percentage of large-budded cells, nuclear position, and spindle orientation. Nuclear position/spindle orientation was scored as abnormal if two separated nuclei were present in the mother of budded cells which were not along the mother/bud axis or if a large-budded cell had a single nucleus, not adjacent to the mother/bud neck. All other configurations were scored as normal. Unbudded cells were additionally scored for the presence of anucleate and multinucleate cells.

```
1    MDQLSDSYAL YNQPVVIDNG SGIIKAGFSG EERPKALEYC LVGNTKYDKV   50
51   MLEGLQGDTF IGNNAQKLRG LLKLRYPIKH GVVEDWDSME LIWSYVLNEV  100
101  LQLQNIGEHP LLITEAPMNP LKNREQMAQV LFETFDVSAL YVSNPAVLSL  150
151  YASGRTTGCV VDCGEGYCST VPIYDGFALP ASMMRMDIGG ADITEQLQFQ  200
201  LRKSAGVSLF SSSEREIVRT MKEKVCYLAK NIKKEEEKYL QGTQDLISTF  250
251  KLPDGRCIEV GNDRYRAPEI LFSPQIIGLG YDGLSDMCMQ SIWKVDLDLR  300
301  KPLLSSIILS GGTTTLKGFG DRMLWDLEAL TKGTSKIKII APSERKYTTW  350
351  IGGSILTGLS TFQRLWTKKS DWLEDSTRVY SNLM                   384
```

Figure 1. The deduced protein sequence of Act3p. Underlined regions indicate residues corresponding to the amplification primers. These sequence data are available from EMBL/GenBank/DDBJ accession number X79811.

Computer-assisted Sequence Analysis

We used the following programs to aid our sequence analysis. BLAST (Altschul et al., 1990); and BESTFIT and PILEUP, both with default parameters (gap length weight = 0.1, gap weight = 3.0) (Genetics Computer Group, 1991).

Results

Cloning of ACT3

We employed a PCR-based approach to identify new actin-related proteins in yeast. The primers were based on sequences which were previously shown to amplify a centractin-like sequence from *Pneumocystis carinii* by L. Fletcher, R. Tidwell, and C. Dykstra (GenBank Accession Number L21184). Using *S. cerevisiae* genomic DNA as a template, we amplified two products. Direct sequencing of the smaller fragment indicated that it represented 24% of the *ACT3* coding region (see Fig. 1). The larger PCR product was not further characterized. The smaller amplification product was subcloned, then used to probe an *S. cerevisiae* genomic library. Two clones were obtained and sequenced, one completely encompassing the other. The larger, 4.5-kb clone was found to contain several open reading frames including *ACT3* and the previously-identified *FUR1* gene which has been mapped to chromosome VIII (Kern et al., 1990). *ACT3* and *FUR1* are convergently transcribed with the predicted polyadenylation signal of *FUR1* residing in the COOH-terminal coding region of *ACT3* (see Fig. 2).

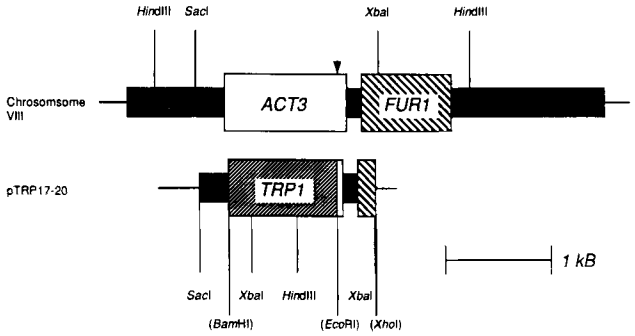

Figure 2. Genomic structure of the *ACT3* and *FUR1* locus and *ACT3* gene replacement strategy. A disruption plasmid was created by cloning *ACT3* flanking sequences adjacent to the *TRP1* gene. The *ACT3* 5′ flanking region is flush with the initiator methionine, while the *ACT3* 3′ flanking region leaves 18 carboxy-terminal residues in order to preserve the *FUR1* polyadenylation signal (*arrowhead*). The replacement accounts for 95% of the *ACT3*-coding region. Restriction sites in parentheses were introduced for the disrupted plasmid construction and do not occur in the genomic sequence.

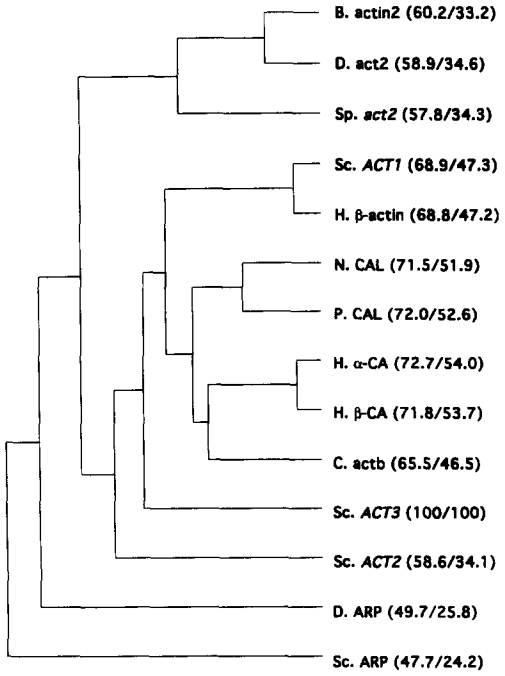

Figure 3. Relationship among members of the ARP family. This dendrogram was created with the aid of the PILEUP program. Percent (similarity/identity) of each ARP to Act3p is noted. Vertical, but not horizontal, distances between branch points reflect relatedness; however, the dendrogram should not be taken as a description of phylogenetic relationships among ARPs. Abbreviations: *B.*, Bovine; *D.*, *D. melanogaster*; *Sp.*, *S. pombe*; *Sc.*, *S. cerevisiae*; *H.*, Human; *N.*, *N. crassa*; *P.*, *P. carinii*; *CAL*, centractin-like protein; *CA*, centractin; *C.*, *C. elegans*.

ACT3 Is Most Related to the Centractin Class of ARPs

To determine the relationship of *ACT3* to known ARPs, we considered both the percent identity, determined by the program BESTFIT, as well as dendrograms and alignments created by the PILEUP program (see Figs. 3 and 4). Most relevant to this study, two ARPs recently identified in the fungi (Edman et al., 1988) *P. carinii* (GenBank Accession Number L21184) and *N. crassa* (Plamann et al., 1994), which by sequence similarity would belong to the centractin class, may be better represented as a class of their own. If conventional actins are taken as a standard for comparison, centractins have a small peptide deletion near residue T229 in Actlp (see Fig. 4). In contrast, *P. carinii* and *N. crassa* centractin-like proteins have small peptide insertions near the position of the centractin deletion (see Fig. 4).

Based on percent identity and similarity, *ACT3* is most closely related to the centractin class of ARPs. However, the dendrogram, which represents the clustering of similarity scores considered pairwise, places *ACT3* both outside the centractin and conventional actin classes. This placement in a unique class is supported by the longer primary sequence of *ACT3* (384 residues) compared to both centractins (376 residues) and conventional actins (375 residues) as well as the distribution of peptide inserts. Specifically, *ACT3* does not share the deletion, relative to conventional actin, found in all centractins near Actlp residue T229 (see Fig. 4). The precise point of the centractin deletion is subjective as this region is divergent from actin. Unlike *ACT1* and *ACT2*, introns were not found in the *ACT3* coding region.

ACT3 Is a Single Copy Gene

Southern hybridization was used to determine if *ACT3* has repeated or related sequences elsewhere in the genome. Genomic DNA prepared from the haploid strain, ABYS1, was independently cleaved with *Eco*RI and *Xba*I. With a probe representing the *ACT3* coding region, a single hybridizing fragment was obtained in each case (Fig. 5). Neither of these fragments comigrated with those hybridizing to an *ACT1* probe. These results are consistent with a single locus representing *ACT3*.

Replacement of the ACT3 Locus with TRP1

To eliminate the expression from the *ACT3* locus, a gene replacement experiment was performed (Fig. 2). A disruption plasmid was created by subcloning the regions flanking the *ACT3* coding sequence into plasmid pBSKS-TRP1 containing the *TRP1* gene. The 3′ flanking region was selected so as to leave the *FUR1* polyadenylation signal intact (Kern et al., 1990), diminishing the possibility of inadvertently affecting *FUR1* expression. This disruption replaced all but the 18 carboxy-terminal residues of Act3p (see Figs. 1 and 2). *act3*Δ1-366::*TRP1* DNA was introduced into two diploid strains, GPY278 and W303. Genomic DNA was prepared from four transformants of each strain and correct integra-

```
Human β-actin          211 DIKEKLCYVALDFEQEMA.......TAASSSSLEKSYELPDGQVITIGNE
S.cerevisiae ACT1      211 DIKEKLCYVALDFEQEMQ.......TAAQSSSIEKSYELPDGQVITIGNE
Human α-centractin     216 AIKERACYLSINPQKDET..........LETEKAQYYLPDGSTIEIGPS
Human β-centractin     216 TIKERACYLSINPQKDEA..........LETEKVQYTLPDGSTLDVGPA
S.cerevisiae ACT3      220 TMKEKVCYLAKNIKKEEEKYLQGTQD......LISTFKLPDGRCIEVGND
N.crassa centractin    214 LIKESVTYVAHDPRKEEKEWAAARMDPA....KIAEYVLPDGNKLKIGAE
P.carinii centractin   215 IIKEKCSYVTLDPRKEEKEWINASISGGKDYTKEEEFKLPDGNVLRLGAE
```

Figure 4. Alignment of selected centractins and conventional actins. This selected region of actin and the actin-related protein centractin indicates peptide insertions (*N. crassa* and *P. carinii*) and deletions (human isoforms) in centractins relative to conventional actins. Note that *ACT3* does not share these features with centractins. The alignment was created with the PILEUP program. The number before each sequence indicates the first amino acid.

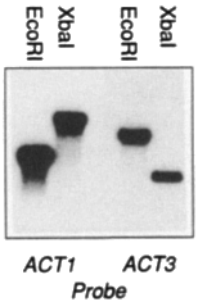

Figure 5. *ACT3* is a single copy gene. A southern analysis of haploid wild-type strain, ABYS1, was made by independent digestion with two restriction enzymes (*Eco*RI, lanes *1* and *3*; and *Xba*I, lanes *2* and *4*). The blot was probed with *ACT1* (lanes *1* and *2*) or *ACT3* (lanes *3* and *4*) and washed at high stringency (0.2× SSC, 65°C). The *ACT3 Eco*RI fragment in lane *3* is ~7.1 kb while the *ACT3 Xba*I fragment in lane *4* is ~3.1 kb.

tion was verified by Southern blotting (Fig 6 *A*). In wild-type genomic DNA, cleavage with *Xba*I yields a 3.1-kb fragment hybridizing to an *ACT3* probe (see Fig. 5, lane *4*). When *TRP1* replaces *ACT3* (see Fig. 2), there is only a small decrease in size of the genomic region, but a new *Xba*I site is introduced, cleaving the 3.1-kB fragment into two smaller fragments (2.4 and 0.7 kb). These fragments hybridize only weakly to the *ACT3* probe, as all but the flanking sequences have been replaced with *TRP1*. Thus, Fig. 6 *A*, lanes *1*, *2*, and *4* contain correct integrants whereas lane *3* does not. Confirmed diploids were sporulated and dissected. Two representative transformants from each strain were sporulated and tetrads were scored for segregation of auxotrophic markers including the Trp+-marked *ACT3* replacement. All transformants sporulated and in 28 tetrads, the Trp+ phenotype segregated 2:2 with no difference in colony size with respect to the Trp phenotype (see Fig. 7).

Genomic DNA and poly(A)+ RNA prepared from tetrad segregants was further evaluated by Southern (Fig. 6 *B*) and northern analysis (Fig. 6, *C* and *D*). The *TRP1* replacement of *ACT3* was found in two of the four spores, as evident by

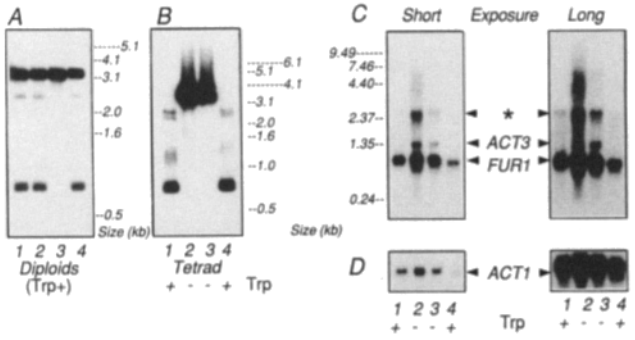

Figure 6. Southern and Northern analysis of parental heterozygous disruptants and their dissected tetrads. (*A*) representative transformants from disruption of parental diploid, W303, cleaved with *Xba*I and probed with *ACT3*. Note that one transformant (lane *3*) is not integrated properly. (*B–D*) lanes *1* and *4* represent the disrupted members of the tetrad. (*B*) genomic DNA prepared from representative tetrad, (BY101-9A, BY101-9B, BY101-9C, BY101-9D) cleaved with *Xba*I and probed with *ACT3*. (*C* and *D*) poly(A)+ RNA (prepared from the same tetrad as *B*) probed with *ACT3* (*C*) or *ACT1* (*D*). Note that the smallest transcript, representing *FUR1*, and the largest transcript (*) are not altered by the disruption when compared to *ACT1* mRNA (*D*). The intermediate-sized transcript, representing *ACT3*, is not present in the Trp+ segregants (lanes *1* and *4*). *ACT1* blots were exposed for 4 h (short exposure) or 35 h (long exposure). *ACT3* blots were exposed for 18 h (short Northern exposure), 26 h (long Northern exposure), or 20 h (Southern).

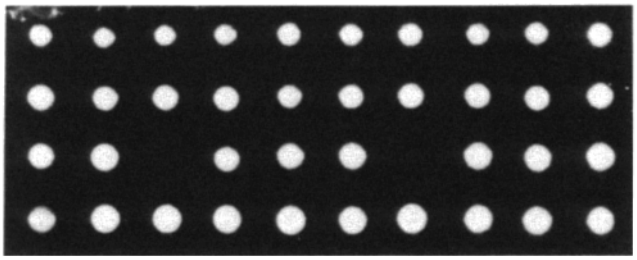

Figure 7. Tetrad dissection of the disrupted heterozygous parental strains. Dissected tetrads, represented here by (BY106), were patched to a master plate, then replica plated for scoring nutritional markers, mating, and growth at temperature and osmotic extremes.

the cleavage of the wild-type 3.1-kb fragment to 2.4- and 0.7-kb disrupted fragments, confirming normal segregation of the disrupted allele. Northern blotting of RNA from segregants uncovered three transcripts hybridizing to the *ACT3* probe (Fig. 6 *C*). The smallest transcript most likely represents *FUR1* as this sequence is represented in the probe and the transcript corresponds well with the published mRNA size (Kern et al., 1990). Considering that the *FUR1* transcript signal is different in each of the four lanes and that ethidium bromide staining of northern RNA had indicated unequal RNA loading (not shown), we made a qualitative assessment of loading differences by reprobing the northern blot with *ACT1* (Fig. 6 *D*). A comparison of the shorter exposure of the *ACT1* northern with the *ACT3* northern confirms that *FUR1* mRNA expression levels are not disturbed by the *act3* disruption. The two remaining transcripts are 1.3 kb and ~2.5 kb. The larger of these transcripts, upon longer exposure, is present in all four segregants of the tetrad and when compared with the *ACT1* RNA signal, is equally represented. This transcript was also found on long exposure when probed with *ACT1* (not shown). As it migrates near the residual 18S rRNA, we probed Northerns prepared with total RNA but found no increased signal strength (data not shown). As the remaining transcript is missing even on long exposures in the segregants which are phenotypically Trp+ and which carry the additional restriction site of *TRP1*, we conclude this transcript represents *ACT3* which is wholly eliminated by the *TRP1* replacement.

Phenotypic Analyses

Cell Growth. Trp+ segregants were found to be competent for mating as judged by replica plating onto a lawn of tester cells. Segregants were inspected for growth on solid media at 14, 30, and 37°C and on hyperosmotic media (1.5 M KCl). Growth rates were also examined in liquid culture at 14, 30, and 37°C (BY103-3A, BY103-8B). Fig. 8 represents the growth of wild-type and *act3*Δ cells at 30 and 14°C. Even after more than four doubling times at 14°C, there is no apparent difference in growth between wild-type and *act3*Δ cells. Growth was also monitored by direct hemocytometer counts and compared with the A_{600}. At 14°C the number of cells per unit A_{600} was 1.5×10^7 (*ACT3*) and 1.3×10^7 (*act3*Δ). These values did not change over the course of the experiment, thus absorbance at 600 nm accurately reflects the increase in cell number for both wild-type and *act3*Δ cells. At all three temperatures, no significant difference in

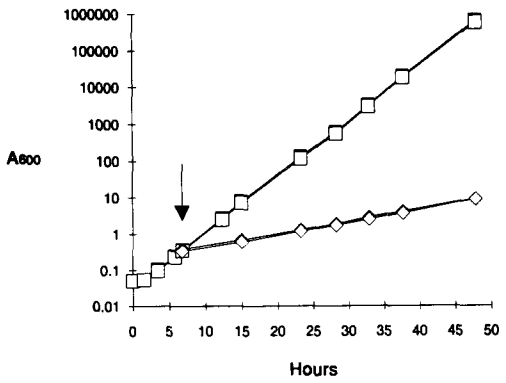

Figure 8. Growth of *ACT3* and *act3Δ* segregants in defined media at 30 and 14°C. Both wild-type and *act3Δ* cells grow at the same rate. Growth was measured by absorbance at 600 nm and confirmed by direct counting with a hemocytometer. Filled characters represent wildtype (*ACT3*), open characters represent *act3Δ*. Squares indicate growth at 30°C, diamonds indicate growth at 14°C. The arrow indicates the point at which part of the 30°C culture was shifted to 14°C.

doubling times was found between haploid strains harboring *ACT3* or *act3Δ*1-366::*TRP1* (see Table IV). However, a subtle but reproducible difference in colony color was evident between *ACT3* and *act3Δ* segregants harboring *ade2* (e.g., BY106-1A, BY106-1B, BY106-1C, and BY106-1D). In 18 out of 20 tetrads, two were dark red, two were light red. The light red color cosegregated with Trp^+ in each case. The two remaining tetrads had three dark red and one light red segregant which cosegregated with Trp^+.

Endocytosis and Vacuolar Morphology. We also examined morphological features of the dissected tetrads grown at 30°C. These included vacuolar morphology/inheritance, visualized by the natural *ade2* fluorophore, and fluid-phase endocytosis visualized by exogenously added Lucifer Yellow. When cells harboring *ade2* are grown in low adenine medium they accumulate a fluorescent polymer in the vacuole (Weisman et al., 1987). Using this natural marker, we examined vacuolar morphology in wild-type and *act3Δ* cells (e.g., BY103-7C, BY103-7D, BY106-9B, BY106-9C, BY108-4B, and BY108-4C). We found no difference in gross vacuolar morphology nor in the inheritance of vacuoles (not shown). As a time, temperature, and energy-dependent marker of fluid-phase endocytosis, and as a secondary measure of vacuolar morphology, we monitored accumulation of Lucifer Yellow in wildtype and *act3Δ* segregants (e.g., BY103-3A and BY103-8B). As with the *ade2* fluorophore, no differences were found in vacuolar morphology. More importantly, cells lacking Act3p had as strong a vacuolar fluorescence as wildtype indicating a similar accumulation of Lucifer Yellow (data not shown).

Table IV. Doubling Time of Wildtype and act3Δ Strains

Growth temperature	Doubling time	
	ACT3	*act3Δ*
	min	
14°C	538	526
30°C	116	117
37°C	128	132

Nuclear Position and Spindle Orientation. To examine nuclear position in *act3Δ* and *ACT3* strains at 14 and 30°C, log-phase cultures, grown at 30°C, were shifted to 14°C for at least 24 h or left at 30°C. Samples were removed, fixed, and stained with DAPI to visualize nuclei. At 30°C, nuclear positioning and division appeared normal in wildtype segregants (e.g., BY103-3A, BY101-9B, and BY106-1D) whereas *act3Δ* segregants had an increased number of abnormally positioned nuclei (e.g., BY101-9A, BY103-8B, and BY106-1C) (see Table V). At 14°C it was readily apparent that *act3Δ*, but not *ACT3* segregants, had an increased percentage of large-budded cells with separated nuclei still in the mother (see Fig. 9 and Table V). The decreased temperature nearly doubled the percentage of cells with abnormal nuclear position. Surprisingly though, anucleate and multinucleate cells were not prevalent under any conditions (see Table V). More interestingly, immunofluorescence with anti-tubulin antibodies indicated that the spindle separating the nuclei was often perpendicular to, or otherwise not in line with, the mother/bud axis (see Fig. 9). In addition, astral microtubules often extended around the periphery of the cell. In other cases, spindle microtubules were fully extended causing the spindle to bend to fit within the confines of the mother cell.

Discussion

Considering that *S. cerevisiae ACT1* and *ACT2*, *Schizosaccharomyces pombe act2*, and *S. cerevisiae* ARP (Harata et al., 1994) are all essential genes, it is most surprising that *ACT3* is nonessential; yet, this is consistent with the phenotype of yeast lacking cytoplasmic dynein (Eshel et al., 1993; Li et al., 1993; Plamann et al., 1994; and see below). The fortuitous location of *ACT3*, adjacent to the *FUR1* locus has allowed us to locate *ACT3* on chromosome VIII. As both *ACT1* (chromosome VI) and *ACT2* (chromosome IV) reside on other chromosomes, apparently these actin-related pro-

Table V. Comparison of Nuclear Migration in ACT3 and act3Δ Strains

Segregant	Growth temperature	Total cells	Large budded cells	Binucleate cells	Anucleate cells	Cells with abnormal nuclear position	Percentage of large budded cells with abnormal nuclei
ACT3	30°C	498	79	1	0	2	3%
act3Δ	30°C	679	151	0	1	28	22%
ACT3	14°C	857	188	0	1	5	3%
act3Δ	14°C	1,384	220	0	3	89	40%

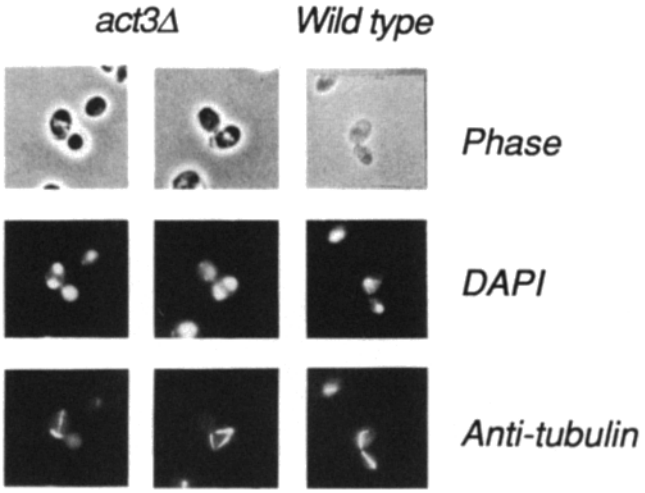

Figure 9. Abnormal spindle orientation and morphology in *act3Δ* segregants. Yeast were grown at 30°C then shifted to 14°C for 24 h. Fixed yeast were stained with a monoclonal antibody against yeast tubulin and with DAPI to visualize nuclei. The spindle morphology of a wild-type segregant is shown for comparison wherein the spindle extends through the bud neck with a single DAPI-stained region in both the mother and bud. The cells labeled *act3Δ* also have elongated spindles separating the DAPI-stained regions, but the entire structure is contained within the mother cell. In some cases, the spindle microtubules extended to their full lengths, resulting in a bent spindle while in other cells, the astral microtubules were greatly extended (not shown).

teins did not arise by simple duplication at a single locus. Assignment based solely on percent identity and similarity suggest *ACT3* is the yeast homologue of vertebrate centractins (52% identity with human centractin). However, two pieces of evidence make such an assignment appear tenuous. First, all known centractins are 376 residues in length and have a small peptide deletion relative to conventional actins. Act3p, like Actlp, does not share the deletion found in centractins. Moreover, Act3p lacks the insertions found in *S. pombe act2* and *S. cerevisiae ACT2* which are maintained in their multicellular homologues (Fyrberg and Fyrberg, 1993). A dendrogram of the ARP family and consideration of peptide insertions and deletions, places *ACT3* clearly outside the centractin class of ARPs. On the other hand, the similarity to the nuclear migration/spindle orientation defect found in dynein mutants suggests Act3p and cytoplasmic dynein are involved in the same cellular process. This in turn suggests a functional relationship with vertebrate centractins (see below). Our search for phenotypic alterations in strains bearing the *act3* deletion included temperature extremes and high osmolarity, a condition known to exacerbate some *ACT1* mutations (Novick and Botstein, 1985; Wertman et al., 1992). As segregation of nutrient markers and their complementation by mating proved normal, we conclude there are no gross aberrations in chromosome segregation or mating.

Northern analysis indicated three transcripts hybridizing to the *ACT3* probe. The largest is not easily accounted for. It migrates close to the position of 18S rRNA, but the lack of an increased signal on total RNA Northerns argues that it is not 18S rRNA. Long exposures of *ACT1*-probed poly(A)$^+$ Northerns revealed an RNA of this size. Southern blotting with *ACT1* and *ACT3* did not reveal additional fragments, suggesting that cross hybridization to a related ARP sequence on Northerns could be the result of the slightly higher T_m of DNA:RNA versus DNA:DNA hybrids. Lastly, other open reading frames were found in the *ACT3* vicinity in addition to *FUR1*. Though they are not well represented in the probe and their size is small in comparison to this RNA species, it remains a formal possibility that the largest transcript stems from an adjacent ORF.

Vertebrate centractins are a component of the p150^{Glued}/dynactin complex involved in the regulation of cytoplasmic dynein (Lees-Miller et al., 1992*b*; Paschal et al., 1993). Thus, in this context, centractins play a role in the regulation of cytoplasmic dynein. The role of cytoplasmic dynein has recently been investigated in the yeast *S. cerevisiae* by disruption (Eshel et al., 1993; Li et al., 1993), where it was found to be nonessential, yet produced a nuclear migration/spindle orientation phenotype. In addition, the elimination of a novel gene, *JNM1*, has also been found to produce a defect similar to *dyn1/dhc1*. Jnmlp is found at the spindle pole, the yeast equivalent of the centrosome, and is proposed to be a component of the dynein microtubule motor (McMillan and Tatchell, 1994). It is interesting to note that a *N. crassa* centractin-like gene has also been reported to have an abnormal nuclear distribution (Plamann et al., 1994). Accordingly, we examined nuclear positioning in *act3Δ* strains and found a striking similarity with the *dhc1/dyn1* phenotype. In cells lacking Act3p, the spindle elongates normally, but entirely within the mother cell, sometimes bending to adopt its full-length. Initially the spindle is not oriented along the mother/bud axis but must eventually pass through the bud neck prior to cytokinesis, in that anucleate and multinucleate cells are not common. Thus, it may well be that despite differences in the overall sequences of Act3p and centractins, these proteins may nonetheless be functionally homologous.

It is worth noting that a similar nuclear positioning phenotype is found in yeast harboring mutations in actin or tubulin; however, there are differences. Specifically, the *act1-4*, temperature-sensitive mutation leads to the creation of a large percentage of binucleate cells at the nonpermissive temperature, a phenotype not found in *DYN1/DHC1* nor *ACT3* mutants. *tub2-401* leads to a selective loss of astral microtubules at 18°C (Sullivan and Huffaker, 1992) and a spindle misorientation phenotype; however, this produces multinucleate and anucleate cells with a concomitant increase in chromosome loss not found in *DYN1/DHC1* nor *ACT3* mutants.

An important difference between mutations in *ACT1*, *TUB2*, *DYN1/DHC1*, *JNM1*, and *ACT3* is that cells lacking Act3p do not have an increased doubling time relative to wild-type cells. In the case of *act1* and *tub2*, it is clear that cytokinesis does not pause for the correction of spindle orientation and binucleate/anucleate cells are produced (Palmer et al., 1992; Sullivan and Huffaker, 1992). On the other hand mutations in *DHC1/DYN1* or *JNM1* do not result in binucleate/anucleate cells, but, at least in the case of *JNM1*, accumulate large-budded cells. In this case cytokinesis apparently pauses while the spindle reorients, leading to an increased doubling time in mutant cells (McMillan and Tatchell, 1994). *act3* is similar to *dhc1/dyn1* and *jnm1* in that anucleate and binucleate cells are not prevalent. Thus, it can be inferred that the cells must eventually reorient their spindle prior to cytokinesis. Surprisingly, however, *act3Δ* cells

do not have an increased doubling time as compared with wildtype and large budded cells do not accumulate. A similar situation has been found in yeast cells lacking dynein by one group (Eshel et al., 1993) but a second group has found conflicting data (Li et al., 1993). How a population of cells with misoriented spindles can have a normal doubling time without producing anucleate or binucleate cells is not clear at this time.

Considering also that the vertebrate endocytic pathway requires cytoplasmic dynein and microtubules (Bomsel et al., 1990; Aniento et al., 1993) and that yeast vacuolar integrity depends on intact microtubules (Guthrie and Wickner, 1988), ARPs which interact with dynein or the cytoskeleton might lead to defects in endocytosis or vacuolar morphology when absent. Analysis of fluid phase endocytosis and vacuolar morphology failed to reveal any differences in strains lacking Act3p. This may be a reflection of the use of actin, not tubulin for endocytosis in yeast (Kubler and Riezman, 1993). The subtle color change we noted in *ade2act3Δ* segregants may reflect a change in vacuolar morphology or function but we believe it is more likely to be due to the biochemical intersection of the tyrptophan and adenine biosynthetic pathways. It is conceivable that the presence of *TRP1* in *act3Δ* segregants could drain substrates, such as phosphoribosylpyrophosphate, from the adenine biosynthesis pathway (Jones and Fink, 1982) decreasing the accumulation of the fluorophore, poly(ribosylaminoimidazole).

The prospect of a yeast centractin homologue opens new avenues of investigation concerning centractin function. Making the most of the genetic tractability of yeast, homologues of the p150^{Glued}/dynactin complex polypeptides or other interacting proteins can be identified. Furthermore, genetic interaction with the actin and tubulin cytoskeletons as well as cytoplasmic dynein can be analyzed. It is worth noting that synthetic lethality is not observed between *dhc1/dyn1* and *jnm1*, yet double mutants harboring either *jnm1* or *dhc1/dyn1* and *cin8*, a kinesin-like protein, do result in lethality (McMillan and Tatchell, 1994). Finally, it will be most interesting to determine, through biochemistry and immunocytochemistry, if Act3p, like vertebrate centractins, is found primarily in a 20S cytosolic complex or associated with the spindle pole body.

We are grateful to L. Fletcher and C. Dykstra for the *P. Carinii* centractin-like ARP primer and protein sequences prior to publication; M. Grunstein for the yeast genomic library; G. Payne for strains GPY278, W303, GX3087, and GX3088, and Y. Sun for suggestions on genomic PCR. Plentiful technical advice was provided by all members of the Payne lab, but in particular, G. Payne for experimental design and tetrad dissection; T. Nicholson and L. Weisman for advice on the *ade2* endogenous fluorophore and hyperosmotic media; and M. Seeger and K. Wilsbach for advice on yeast immunofluorescence and sporulation. Finally, we thank Andy Jacobson for assistance with the confocal microscopy.

This work was supported by the family of Libbie Goldman under the auspices of the Jonsson Cancer Center Foundation and the Margaret E. Early Medical Research Trust. D. I. Meyer acknowledges support from the American Cancer Society and S. W. Clark from a U.S. Public Health Service Molecular and Cell Biology Training grant GM07185.

Received for publication 13 June 1994 and in revised form 27 June 1994.

References

Altschul, S. F., W. Gish, W. Miller, E. W. Myers, and D. J. Lipman. 1990. Basic local alignment search tool. *J. Mol. Biol.* 215:403–410.

Aniento, F., N. Emans, G. Griffiths, and J. Gruenberg. 1993. Cytoplasmic dynein-dependent vesicular transport from early to late endosomes. *J. Cell Biol.* 123:1373–1387.

Ausubel, F. M., R. Brent, R. E. Kingston, D. D. Moore, J. G. Seidman, J. A. Smith, and K. Struhl. 1993. *Current Protocols in Molecular Biology.* John Wiley & Sons, Inc. New York.

Bomsel, M., R. Parton, A. Kuznetsov, T. A. Schroer, and J. Gruenberg. 1990. Microtubule- and motor-dependent fusion in vitro between apical and basolateral endocytic vesicles from MDCK cells. *Cell.* 62:719–731.

Bork, P., C. Sander, and A. Valencia. 1992. An ATPase domain common to prokaryotic cell cycle proteins, sugar kinases, actin, and hsp70 heat shock proteins. *Proc. Natl. Acad. Sci. USA.* 89:7290–7294.

Clark, S. W., and D. I. Meyer. 1992. Centractin is an actin homologue associated with the centrosome. *Nature (Lond.).* 359:246–250.

Clark, S. W., and D. I. Meyer. 1993. Long lost cousins of actin. *Curr. Biol.* 3:54–55.

Edman, J. D., J. A. Kovacs, H. Masur, D. V. Santi, H. J. Elwood, and M. L. Sogin. 1988. Ribosomal RNA sequence shows *Pneumocystis carinii* to be a member of the Fungi. *Nature (Lond.).* 334:519–522.

Eshel, D., L. A. Urrestarazu, S. Vissers, J.-D. Jauniaux, J. C. van Vliet-Reedijk, R. J. Planta, and I. R. Gibbons. 1993. Cytoplasmic dynein is required for normal nuclear segregation in yeast. *Proc. Nat. Acad. Sci. USA.* 90:11172–11176.

Flaherty, K. M., D. B. McKay, W. Kabsch, and K. C. Holmes. 1991. Similarity of the three-dimensional structures of actin and the ATPase fragment of a 70-kDa heat shock cognate protein. *Proc. Nat. Acad. Sci. USA.* 88: 5041–5045.

Fletcher, L. D., R. R. Tidwell, and C. C. Dykstra. 1993. Cloning and characterization of an actin II gene from *Pneumocystis carinii* which encodes a centractin-like protein. GenBank accession number L21184.

Frankel, S., M. B. Heintzelman, S. Artavanis-Tsakonas, and M. S. Mooseker. 1994. Identification of a divergent actin-related protein in *Drosophila. J. Mol. Biol.* 235:1351–1356.

Fyrberg, C., and E. Fyrberg. 1993. A *Drosophila* homologue of the *Schizosaccharomyces pombe act2* gene. *Biochem. Genet.* 31:329–341.

Gallwitz, D., and I. Sures. 1980. Structure of a split yeast gene: complete nucleotide sequence of the actin gene in *saccharomyces cerevisiae. Proc. Nat. Acad. Sci. USA.* 77:2546–2550.

Garen, S. H., and D. R. Kankel. 1983. Golgi and genetic mosaic analyses of visual system mutants in *Drosophila melanogaster. Dev. Biol.* 96:445–466.

Genetics Computer Group. 1991. GCG Package, Program Manual. Version 7. Madison, WI.

Gill, S. R., T. A. Schroer, I. Szilak, E. R. Steuer, M. P. Sheetz, and D. W. Cleveland. 1991. Dynactin, a conserved, ubiquitously expressed component of an activator of vesicle motility mediated by cytoplasmic dynein. *J. Cell Biol.* 115:1639–1650.

Guthrie, B. A., and W. Wickner. 1988. Yeast vacuoles fragment when microtubules are disrupted. *J. Cell Biol.* 107:115–120.

Guthrie, C., and G. R. Fink. 1991. Guide to Yeast Genetics and Molecular Biology. Academic Press, Inc., San Diego. 933 pp.

Harata, M., A. Karwan, and U. Wintersberger. 1994. A new essential gene of *Saccharomyces cerevisiae* coding for an actin-related protein. *Proc. Nat. Acad. Sci. USA.* In press.

Harte, P. J., and D. R. Kankel. 1982. Genetic analysis of mutations at the *Glued* locus and interacting loci in *Drosophila melanogaster. Genetics.* 101:477–501.

Herman, I. M. 1993. Actin isoforms. *Curr. Opin. Cell Biol.* 5:48–55.

Holton, T. A., and M. W. Graham. 1991. A simple and efficient method for direct cloning of PCR products using ddT-tailed vectors. *Nucleic Acid Res.* 19:1156.

Holzbaur, E. L. F., J. A. Hammarback, B. M. Paschal, J. G. Kravit, K. K. Pfister, and R. B. Vallee. 1991. Homology of a 150K cytoplasmic dynein-associated polypeptide with the *Drosophila* gene *Glued. Nature (Lond.).* 351:579–583.

Huffaker, T. C., J. H. Thomas, and D. Botstein. 1988. Diverse effects of β-tubulin mutations on microtubule formation and function. *J. Cell Biol.* 106:1997–2010.

Ito, H., Y. Fukuda, K. Murata, and A. Kimura. 1983. Transformation of intact yeast cells treated with alkali cations. *J. Bacteriol.* 153:163–168.

Jones, E. W., and G. R. Fink. 1982. Regulation of amino acid and nucleotide biosynthesis in yeast. *In* The Molecular Biology of the Yeast *Saccharomyces:* Metabolism and Gene Expression. J. N. Strathern, E. W. Jones, and J. R. Broach, editors. Cold Spring Harbor Laboratory Press, Cold Spring Harbor, NY. 181–299.

Kern, L., J. de Montigny, R. Jund, and F. Lacroute. 1990. The *FUR1* gene of *Saccharomyces cerevisiae*: cloning, structure and expression of wild-type and mutant alleles. *Gene (Amst.).* 88:149–157.

Kubler, E., and H. Riezman. 1993. Actin and fimbrin are required for the internalization step of endocytosis in yeast. *EMBO (Eur. Mol. Biol. Organ.) J.* 12:2855–2862.

Lees-Miller, J. P., G. Henry, and D. M. Helfman. 1992*a*. Identification of *act2*, an essential gene in the fission yeast *Schizosaccharomyces pombe* that encodes a protein related to actin. *Proc. Nat. Acad. Sci. USA.* 89:80–83.

Lees-Miller, J. P., D. M. Helfman, and T. A. Schroer. 1992*b*. A vertebrate actin-related protein is a component of a multisubunit complex involved in

microtubule-based vesicle motility. *Nature (Lond.).* 359:244–246.
Li, Y.-Y., E. Yeh, T. Hays, and K. Bloom. 1993. Disruption of mitotic spindle orientation in a yeast dynein mutant. *Proc. Nat. Acad. Sci. USA.* 90: 10096–10100.
McMillan, J. N., and K. Tatchell. 1994. The *JNM1* gene in the yeast *saccharomyces cerevisiae* is required for nuclear migration and spindle oritentation during the mitotic cell cycle. *J. Cell Biol.* 125:143–158.
Melki, R., I. E. Vainberg, R. L. Chow, and N. J. Cowan. 1993. Chaperonin-mediated folding of vertebrate actin-related protein and γ-tubulin. *J. Cell Biol.* 122:1301–1310.
Meyerowitz, E. M., and D. R. Kankel. 1978. A genetic analysis of visual system development in *Drosophila melanogaster. Dev. Biol.* 62:112–142.
Munn, A. L., L. Silveira, M. Elgort, and G. S. Payne. 1991. Viability of clathrin heavy-chain-deficient *Saccharomyces cerevisiae* is compromised by mutations at numerous loci: implications for the suppression hypothesis. *Molec. Cell Biol.* 11:3868–3878.
Novick, P., and D. Botstein. 1985. Phenotypic analysis of temperature-sensitive yeast actin mutants. *Cell.* 40:405–416.
Palmer, R. E., D. S. Sullivan, R. Huffaker, and D. Koshland. 1992. Role of astral microtubules and actin in spindle orientation and migration in the budding yeast, *Saccharomyces cerevisiae. J. Cell Biol.* 119:583–593.
Paschal, B. M., E. L. F. Holzbaur, K. K. Pfister, S. Clark, D. I. Meyer, and R. B. Vallee. 1993. Characterization of a 50-kDa polypeptide in cytoplasmic dynein preparations reveals a complex with p150^{GLUED} and a novel actin. *J. Biol. Chem.* 268:15318–15323.
Pierre, P., J. Scheel, J. E. Rickard, and T. E. Kreis. 1992. CLIP-170 links endocytic vesicles to microtubules. *Cell.* 70:887–900.
Plamann, M., P. F. Minke, J. H. Tinsley, and K. Bruno. 1994. Neurospora mutants defective in cytoplasmic dynein or centractin have abnormal nuclear distribution. *J. Cell Biol.* 127:139–149.
Pollard, T. D., and J. A. Cooper. 1986. Actin and actin-binding proteins. A critical evaluation of mechanisms and functions. *Annu. Rev. Biochem.* 55: 987–1035.
Rose, M. D., F. Winston, and P. Hieter. 1990. *Methods in yeast genetics: a laboratory course manual.* Cold Spring Harbor Laboratory Press, Cold Spring Harbor, NY. 198 pp.
Sambrook, S., E. F. Fritsch, and T. Maniatis. 1989. *Molecular Cloning: A Laboratory Manual.* 2nd ed. Cold Spring Harbor Laboratory Press, Cold Spring Harbor, NY.
Sawin, K. E., and J. M. Scholey. 1991. Motor proteins in cell division. *Trends Cell Biol.* 1:123–129.
Schroer, T. A., and M. P. Sheetz. 1991. Two activators of microtubule-based vesicle transport. *J. Cell Biol.* 115:1309–1318.
Schroer, T. A., E. R. Steuer, and M. P. Sheetz. 1989. Cytoplasmic dynein is a minus end-directed motor for membranous organelles. *Cell.* 56:937–946.
Schwob, E., and R. P. Martin. 1992. New yeast actin-like gene required late in the cell cycle. *Nature (Lond.).* 355:179–182.
Schwob, E., G. Alt, S. Andres, G. Dirheimer, and R. P. Martin. 1988. *ACT2,* a novel yeast split gene coding for an actin-like protein. *Yeast.* 4(Suppl.): 108.
Sullivan, D. S., and T. C. Huffaker. 1992. Astral microtubules are not required for anaphase B in *Saccharomyces cerevisiae. J. Cell Biol.* 119:379–388.
Tanaka, T., F. Shibasaki, M. Ishikawa, N. Hirano, R. Sakai, J. Nishida, T. Takenawa, and H. Hirai. 1992. Molecular cloning of bovine actin-like protein, actin2. *Biochem. Biophys. Res. Commun.* 187:1022–1028.
Toyn, J., A. R. Hibbs, P. Sanz, J. Crowe, and D. I. Meyer. 1988. *In vivo* and *in vitro* analysis of *ptl1,* a yeast *ts* mutant with a membrane-associated defect in protein translocation. *EMBO (Eur. Mol. Biol. Organ.) J.* 7: 4347–4353.
Volgelstein, B. 1987. Rapid purification of DNA from agarose gels by centrifugation through a disposable plastic column. *Anal. Biochem.* 160:115– 118.
Weisman, L. S., R. Bacallao, and W. Wickner. 1987. Multiple methods of visualizing the yeast vacuole permit evaulation of its morphology and inheritance during the cell cycle. *J. Cell Biol.* 105:1539–1547.
Wertman, K. F., D. G. Drubin, and D. Botstein. 1992. Systematic mutational analysis of the yeast *ACT1* gene. *Genetics.* 132:337–350.